Physics of the Earth and Planetary Interiors 232 (2014) 57–60

Contents lists available at ScienceDirect

Physics of the Earth and Planetary Interiors

journal homepage: www.elsevier.com/locate/pepi

# Influence of oxygen fugacity on the electrical conductivity of hydrous olivine: Implications for the mechanism of conduction

Lidong Dai [a,b], Shun-ichiro Karato [b,*]

[a] Laboratory for High Temperature and High Pressure Study of the Earth's Interior, Institute of Geochemistry, Chinese Academy of Sciences, Guiyang, Guizhou 550002, China
[b] Department of Geology and Geophysics, Yale University, New Haven, CT 06511, USA

ARTICLE INFO

*Article history:*
Received 5 December 2013
Received in revised form 27 March 2014
Accepted 9 April 2014
Available online 5 May 2014

*Keywords:*
Oxygen fugacity
Electrical conductivity
Hydrogen
Olivine

ABSTRACT

Various mechanisms of hydrogen-assisted electrical conductivity predict different dependence of conductivity on oxygen fugacity. If a majority of hydrogen-related defects (i.e., two protons at M-site) carries the electrical current, then the conductivity will be independent of oxygen fugacity, whereas if a minority defect such as free proton carries the electrical conductivity, then the electrical conductivity will decrease with oxygen fugacity. We have determined the dependence of hydrogen-assisted electrical conductivity on oxygen fugacity in hydrous olivine. We found that the hydrogen-assisted electrical conductivity in olivine decreases with oxygen fugacity. This result supports a model where hydrogen-related defect with minor concentration (e.g., free proton or one hydrogen at M-site) carries most of the electric charge.



## 1. Introduction

Importance of hydrogen in electrical conductivity in minerals such as olivine was pointed out by (Karato, 1990). This model was motivated by the reported high diffusion coefficient of hydrogen (Mackwell and Kohlstedt, 1990) and known appreciable solubility of hydrogen. Recent experimental studies have largely confirmed this model (e.g., Karato and Wang, 2013; Yoshino and Katsura, 2013), but some details are still debated.

One of the most important observations is the large discrepancies between the results of H-D isotope diffusion (Du Frane and Tyburczy, 2012) and electrical conductivity. (Karato, 2013) developed a theory of isotope diffusion and discussed that such discrepancies can be explained if electrical conductivity is due mostly to defects with small concentration (e.g., free proton) but high mobility whereas isotope diffusion is controlled by the diffusion of defects slow diffusing species. In contrast to this hybrid model of electrical conductivity, most of other researchers propose a model where all hydrogen atoms contribute equally to electrical conductivity (e.g., Du Frane and Tyburczy, 2012; Yoshino and Katsura, 2013). Although detailed discussions that favor the hybrid model has been published (e.g., Karato, 2006, 2013), it is useful to provide an additional experimental study to test these models.

In this paper, we present the results of an experimental study to determine the dependence of electrical conductivity of olivine on oxygen fugacity under hydrogen-rich conditions. Many experimental studies on electrical conductivity of dry olivine showed that electrical conductivity increases with oxygen fugacity (e.g., Duba and Nicholls, 1973; Schock et al., 1989). This is due to the fact that the concentration of the charge carrying species, i.e., ferric iron, increases with oxygen fugacity. However, the situation can be different when the charge carrier is proton-related defects. Indeed, a defect chemistry analysis on olivine (or other (Mg, Fe), Si bearing minerals) shows that the dependence of conductivity on oxygen fugacity will be different for hydrogen-assisted conductivity. In more detail, if hydrogen-assisted conductivity were due to the most abundant hydrogen-related defects, i.e., $(2H)_M^{\times}$ (two protons at M-site vacancy), then electrical conductivity will be independent of oxygen fugacity, whereas if electrical conductivity is due to minority defects such as $H^{\bullet}$ (free proton) or $H_M'$ (one proton at M-site vacancy), then electrical conductivity would decrease with oxygen fugacity (Nishihara et al., 2008). Therefore a study on the influence of oxygen fugacity will provide a clear means to distinguish among various mechanisms of hydrogen-assisted electrical conduction.

## 2. Experimental procedure

### 2.1. Sample preparation

The hydrous polycrystalline olivine samples were synthesized from San Carlos olivine powders with the grain size less than 5 μm by hydrothermal annealing experiments at $P = 4$ GPa and

* Corresponding author. Tel.: +1 203 432 3147; fax: +1 203 432 3134.
*E-mail address:* shun-ichiro.karato@yale.edu (S.-i. Karato).

http://dx.doi.org/10.1016/j.pepi.2014.04.003
0031-9201/

$T$ = 1473 K for 3 h. About 1.85 wt% of San Carlos orthopyroxene was added to buffer the oxide activity. Powder samples of olivine and orthopyroxene mixture were sealed into a metal capsule (water was added by the dehydration of talc + brucite). Both synthesis and conductivity measurements were performed using the same solid oxygen buffer (e.g., Mo–$MoO_2$, Ni–NiO and Re–$ReO_2$). Our previous experience indicates that under these environments, the oxidation conditions of samples are well buffered by the metal and its corresponding metal oxide reactions (e.g., Nishihara et al., 2006, 2008). The oxygen fugacity was controlled by varying the selected metal type in the electrodes, corresponding sleeves, and shielding cases. The shielding is made of metal foils such as Mo, Ni, Re, whose thickness is 25 μm. After the electrical conductivity measurements were completed, the recovered electrode/sample interfaces were examined by the scanning electron microscope in order to confirm the coexistence of metal and its corresponding metal oxide. We confirmed the co-existence of metal and corresponding metal oxide at the interface between electrode and the samples.

### 2.2. Sample characterization

In order to determine the water content of the samples, the infrared spectra of samples were obtained at wavenumbers from 1000 to 4000 $cm^{-1}$ both before and after each experiment. The measurements were made using a Fourier transform infrared spectroscopy (FT-IR) spectrometer (BIORAD, Varian 600 UMA). Doubly polished samples with a thickness of ~100 μm were prepared for the IR analysis. The IR absorption of samples was measured by unpolarized radiation with a mid-IR light source, a KBr beam splitter and an MCT detector with a 150 × 150 $\mu m^2$ aperture. 256 scans were accumulated for each sample. The infrared spectra of the acquired samples are shown in Fig. 1. We used the (Paterson, 1982) calibration to determine the water content from FT-IR absorption using,

$$C_{OH} = \frac{B_i}{150\xi}\int \frac{K(v)}{(3780 - v)}dv \quad (1)$$

where $C_{OH}$ is the molar concentration of hydroxyl (ppm wt $H_2O$ or H/$10^6$ Si), $B_i$ is the density factor (4.39 × $10^4$ cm H/$10^6$ Si), $\xi$ is the orientation factor (1/3), and $K(v)$ is the absorption coefficient in $cm^{-1}$ at wavenumber $v$ in $cm^{-1}$. The integration was made from 3000 to 3750 $cm^{-1}$. If another calibration such as (Bell et al., 2003) is used, the water content will be larger by a factor of ~3.

The water content of the original sample is less than 8H/$10^6$ Si (0.0001 wt% $H_2O$). After the olivine was annealed under the hydrous environment, one sample containing different water contents of ~180–280 ppm wt was obtained. The water loss during the electrical conductivity measurements of hydrous sample was less than 8% of the total water.

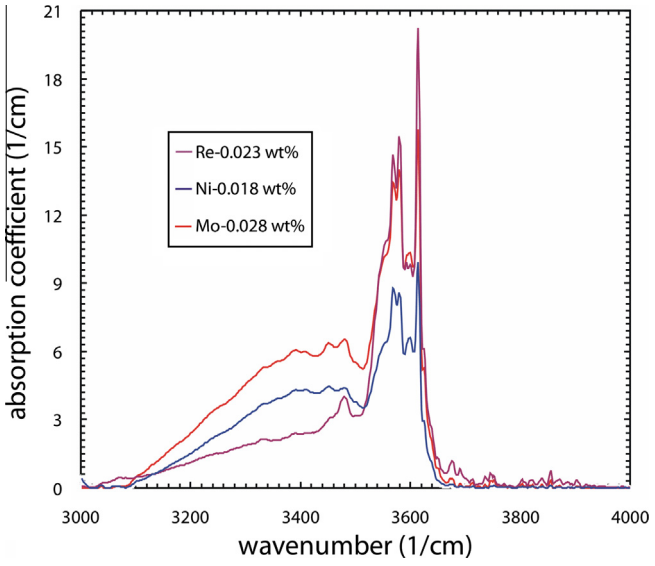


**Fig. 1.** The representative FT-IR spectra of the recovered olivine aggregates after electrical conductivity measurements for the wavenumber range of 3000–4000 $cm^{-1}$.

### 2.3. Impedance spectroscopy measurements

The experimental sample assembly is shown in Fig. 2. Pressure was generated by eight cubic tungsten carbide anvils (26 × 26 × 26 $mm^3$) with an 18 mm truncated edge length. Pressure calibrations were conducted using the phase transitions of coesite to stishovite (Zhang et al., 1996) (9.5 GPa and 1573 K). In order to avoid the influence of adsorbed water on the measurement of electrical conductivity, sample assembly parts including MgO octahedral pressure medium, MgO and $Al_2O_3$ insulation tubes were heated to 1223 K for 15 h prior to each experiment (Mo ring and a sample itself were not heat treated). In order to control the oxygen fugacity of the sample chamber and reduce the leakage currents, a metal foil shield (e.g., Mo, Ni and Re) was placed between a sample and an MgO insulation tube. The metal used for shielding purpose is the same as the metal used for a capsule. A disk-shaped sample (Φ1.6 × 0.4 mm) was placed between two parallel metal electrodes that were surrounded by alumina rings. The temperature was measured by a $W_{5\%}Re$–$W_{26\%}Re$ thermocouple that is attached to another side of metal electrode (metal electrode is in direct contact with a sample, but the thermo-couple is not). The experimental errors of the pressure and temperature gradient were estimated to be no more than 0.5 GPa and 10 K, respectively (absolute error in pressure estimate can be larger but the relative error is ~0.5 GPa or less). The errors in the electrical conductivity measurement through the impedance fitting were estimated to be less than 4%.

The pressure was first raised at the rate of ~0.9 GPa/h to a designated pressure. Under a constant pressure condition, temperature was raised at the rate of ~50 K/min to the preset value and the impedance spectroscopy measurements were performed at various temperatures. After the temperature reached to an each value for a constant pressure condition, the ZPlot program of a Solartron-1260 Impedance/Gain-phase analyzer was run to determine the complex impedance for the frequency range of $f = 10^{-2}$–$10^6$ Hz for a sinusoidal alternating current of signal voltage of 1.0 V. The impedance semi-circle arc of high frequency

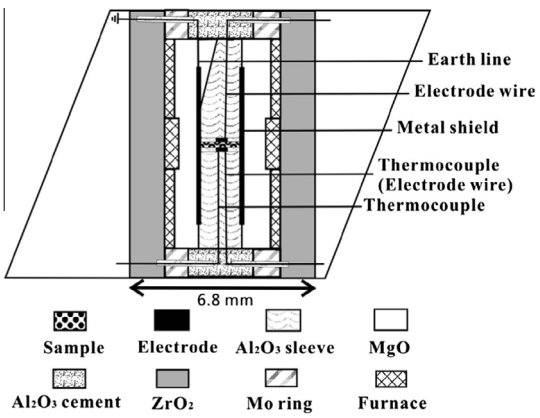


**Fig. 2.** The experimental setup for electrical conductivity measurements at high pressure and temperature.

branch ($10^6$–$10^3$ Hz) was fitted by virtue of an equivalent circuit of the ZView program that was made up of a resistor connected in parallel with a capacitor. From the fitting of the semi-circle to this model, we determined the resistance of a sample, and calculated the electrical conductivity under a given thermodynamic condition. In most of the runs, the conductivity was determined with decreasing temperature after the peak temperature was reached because the temperature becomes more stable in the process of decreasing cycle. All experimental conditions including water content before and after each experiment, pressure and temperature are summarized in Table 1.

## 3. Results

The representative impedance spectroscopy results at conditions of 4 GPa, 873–1273 K and the water content of ~280 ppm wt are shown in Fig. 3. Results obtained under other conditions are qualitatively similar to those illustrated here. We observed two circles at high temperatures, whereas only one circle was observed at low temperatures. The presence of two circles in the impedance spectroscopy implies two processes of charge transfer and blocking. The first circle originated at the origin ($Z' = Z'' = 0$) likely corresponds to a parallel combination of resistor and capacitor, and the second circle likely represents the conduction process between sample and electrode (Barkmann and Cemič, 1996; Tyburczy and Roberts, 1990). The presence of a capacitor in the impedance response implies that there are mechanisms to accumulate electric charge in the sample (e.g., grain-boundaries) or at the sample/electrode interface.

The electrical conductivities of the samples were calculated using the following equation,

$$\sigma = \frac{L/S}{R} = \frac{L}{SR} \tag{2}$$

where $L$ is the sample length and $S$ is the cross section area of the electrode. Both $L$ and $S$ are determined before and after each experiment and only small changes in $L$ and $S$ are observed (less than 3%). The relationship between the electrical conductivity and temperature under different oxygen fugacities was analyzed assuming the following relation,

$$\sigma = A \cdot C_w^r \cdot f_{O_2}^q \cdot \exp\left(-\frac{H^*}{RT}\right) \tag{3}$$

where $A$, $q$ are the constants, $C_w$ is the water content, $r$ is a constant (~0.62) that is provided by Wang et al. (2006), $f_{O_2}$ is the oxygen fugacity, $H^*$ is the activation enthalpy, $T$ is the temperature and $R$ is the gas constant.

In order to obtain the oxygen fugacity exponent, $q$, we compared the results from different oxygen fugacity buffer at the same water content using the value of $r$ (=0.62) after (Wang et al., 2006). The results are summarized in Fig. 4. The fitted parameter values for electrical conductivity of hydrous wadsleyite are list in Table 2. With increasing oxygen fugacity from the solid buffer along Mo–$MoO_2$, Ni–NiO to Re–$ReO_2$, the electrical conductivity of hydrous polycrystalline olivine decreases at the same temperature and pressure.

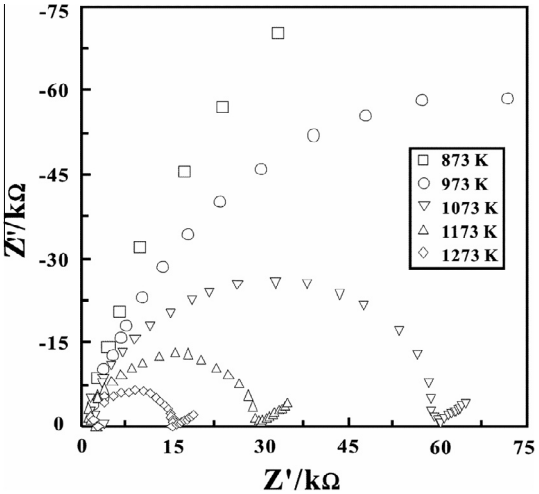


**Fig. 3.** A $Z'$ vs. $Z''$ plot of complex impedance of hydrous olivine aggregates from $10^{-2}$ to $10^6$ Hz (right to left), obtained under conditions of 4.0 GPa, 873–1273 K and controlled oxygen fugacity by Mo–$MoO_2$ solid buffer with a 280 ppm wt water content. $Z'$ and $Z''$ are the real and imaginary part of complex impedance respectively.

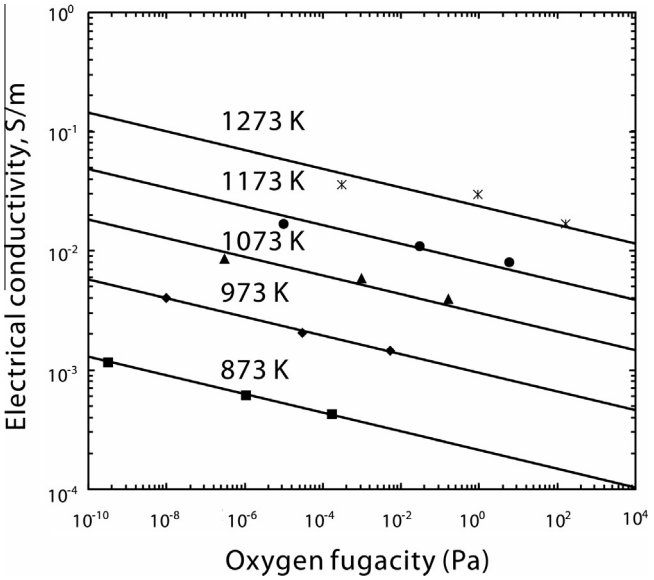


**Fig. 4.** Influence of oxygen fugacity on the electrical conductivity of hydrous olivine aggregates under conditions of 4.0 GPa, 873–1273 K, 280 ppm wt water content and three different solid buffers (e.g., Mo–$MoO_2$, Ni–NiO and Re–$ReO_2$).

## 4. Discussion

Our results for olivine are similar to those for wadsleyite (Dai and Karato, 2009) where electrical conductivity of hydrous samples decreases with the increase of oxygen fugacity. On average, the oxygen fugacity exponent ($q$) is $-0.066 \pm 0.007$. However, in more detail, the absolute value of $q$ decreases with temperature.

**Table 1**
Summary of runs.

| Run No. | $P$ (GPa) | $T$ (K) | Oxygen buffers | Water content ($H/10^6$ Si) | |
|---|---|---|---|---|---|
| | | | | Before experiment | After experiment |
| K1403 | 4 | 873–1273 | Re–$ReO_2$ | 3675 | 3628 |
| K1398 | 4 | 873–1473 | Ni–NiO | 2853 | 2737 |
| K1400 | 4 | 873–1473 | Mo–$MoO_2$ | 4406 | 4349 |

**Table 2**
The fitted parameters in equation (3) for hydrous olivine aggregates under conditions of 4.0 GPa and controlled oxygen buffers (Re–$ReO_2$, Ni + NiO and Mo + $MoO_2$). The fitted parameters, $\sigma_0$ and $H^*$ correspond to the water content of our sample (280 ppm wt based on the Paterson calibration, 840 ppm wt based on the SIMS calibration).

| Oxygen buffers | $T$ (K) | $\mathrm{Log}_{10}\ \sigma_0$ (S/m) | $H^*$ (kJ/mol) |
|---|---|---|---|
| Re–$ReO_2$ | 873–1273 | 1.67 ± 0.08 | 85 ± 5 |
| Ni–NiO | 873–1273 | 2.00 ± 0.13 | 88 ± 3 |
| Mo–$MoO_2$ | 873–1273 | 1.69 ± 0.10 | 78 ± 4 |

**Table 3**
The fitted parameter ($q$) for hydrous olivine aggregates under conditions of 4.0 GPa, 280 ppm wt water content and controlled oxygen buffers (Re–$ReO_2$, Ni + NiO and Mo + $MoO_2$).

| $T$ (K) | $q$ |
|---|---|
| 873 | −0.080 ± 0.02 |
| 973 | −0.079 ± 0.03 |
| 1073 | −0.060 ± 0.01 |
| 1173 | −0.058 ± 0.02 |
| 1273 | −0.055 ± 0.01 |

We interpret this result assuming that the oxygen fugacity dependence of electrical conductivity is due to the dependence of number density of charge carrier on oxygen fugacity. The defect chemistry of hydrous olivine aggregates indicates that the concentration of defects [$X$] depends on the chemical environment as (e.g., Karato, 2008; Nishihara et al., 2008):

$$[X] \propto f_{H_2O}^{p} \times f_{O_2}^{q} \times a_{MeO}^{s} \quad (4)$$

where $p$, $q$ and $s$ are constants that are dependent on different defect types; $f_{H_2O}^{p}$ is the water fugacity, $f_{O_2}$ is the oxygen fugacity; $a_{MeO}$ $a$ is the activity of the metal oxide (MeO) (see Table 3).

The observed values of exponential factors of $q$ (−0.066) are close to the results (−0.058) obtained by Dai and Karato (2009) for hydrous wadsleyite in the mantle transition zone under conditions of 15 GPa, 873–1273 K, and with three solid buffers (Ni + NiO, Mo + $MoO_2$ and Re + $ReO_2$). These values are different from those for anhydrous olivine where conduction occurs through the migration of iron-related defects (“polaron”) (Schock et al., 1989). The observed negative oxygen fugacity exponent is consistent with conductivity mechanisms involving protons. However, the observed results showing the value of $q$ (−0.066) means that the dominant hydrogen-related defect of independent oxygen fugacity, $2(H)_M^{\times}$, is not the main charge carrier (for this defect, $q = 0$). Instead, some ionized defects such as $H_M'$ with the charge neutrality condition of $[Fe_M^{\bullet}] = 2[V_M'']$ (this model predicts $r = 1/2$ and $q = -1/12$) or $H^{\bullet}$ with the charge neutrality condition of $[Fe_M^{\bullet}] = [H_M']$ this model predicts $r = 3/4$ and $q = -1/8$) is a plausible model (Karato, 2008). These minority defects could control electrical conductivity if their mobility is high. Again, however, the absolute value of $q$ (−0.066) is less than those model predictions. A possible explanation is that under the experimental conditions, two (or more) conduction mechanisms might operate. In fact, (Dai and Karato, 2014) presented evidence that conduction mechanism of hydrous olivine changes from free proton mechanism to two proton at M-site mechanism as temperature increases. If such a transition in mechanism were to occur, then one would expect that the absolute value of $q$ decreases with the increase of temperature. We interpret that the temperature dependence of $q$ observed in our experiment is consistent with this model. An alternative possibility is that a sample is not completely equilibrium with the oxygen fugacity buffer at low temperatures. This possibility cannot be ruled out, but a sample is likely in chemical equilibrium at least in the cooking stage before the conductivity measurements.

We conclude that hydrogen-assisted conductivity in olivine decreases with increasing oxygen fugacity. This is inconsistent with a model where all hydrogen atoms contribute equally to electrical conductivity. Therefore our new results provide additional support for a hybrid model of electrical conductivity developed by Karato (2006, 2013).

## Acknowledgments

George Amulele and Zhenting Jiang provided technical assistance in the FT-IR measurement. Zhenting Jiang conducted the SEM analyses of the recovered samples. This research was financially supported by the “135” Program of Institute of Geochemistry, CAS and NSF of China (41174079) and partly by NSF of United States.

## References

Barkmann, T., Cemič, L., 1996. Impedance spectroscopy and defect chemistry of fayalite. Phys. Chem. Miner. 23, 186–192.
Bell, D.R., Rossman, G.R., Maldener, J., Endisch, D., Rauch, F., 2003. Hydroxide in olivine: a quantitative determination of the absolute amount and calibration of the IR spectrum. J. Geophys. Res. 108. http://dx.doi.org/10.1029/2001JB000679.
Dai, L., Karato, S., 2009. Electrical conductivity of wadsleyite under high pressures and temperatures. Earth Planet. Sci. Lett. 287, 277–283.
Dai, L., Karato, S., 2014. Highly anisotropic electrical conductivity of the asthenosphere caused by hydrogen diffusion in olivine. Proc. Natl. Acad. Sci. USA, submitted for publication.
Du Frane, W.L., Tyburczy, J.A., 2012. Deuterium–hydrogen interdiffusion in olivine: implications for point defects and electrical conductivity. Geochem. Geophys. Geosyst. 13. http://dx.doi.org/10.1029/2011GC003895.
Duba, A., Nicholls, I.A., 1973. The influence of oxidation state on the electrical conductivity in olivine. Earth Planet. Sci. Lett. 18, 59–64.
Karato, S., 1990. The role of hydrogen in the electrical conductivity of the upper mantle. Nature 347, 272–273.
Karato, S., 2006. Influence of hydrogen-related defects on the electrical conductivity and plastic deformation of mantle minerals: a critical review. In: Jacobsen, S.D., van der Lee, S. (Eds.), Earth's Deep Water Cycle. American Geophysical Union, Washington, DC, pp. 113–129.
Karato, S., 2008. Deformation of Earth Materials: Introduction to the Rheology of the Solid Earth. Cambridge University Press, Cambridge.
Karato, S., 2013. Theory of isotope diffusion in a material with multiple-species and its implications for hydrogen-enhanced electrical conductivity in olivine. Phys. Earth Planet. Inter. 219, 49–54.
Karato, S., Wang, D., 2013. Electrical conductivity of minerals and rocks. In: Karato, S. (Ed.), Physics and Chemistry of the Deep Earth. Wiley-Blackwell, New York, pp. 145–182.
Mackwell, S.J., Kohlstedt, D.L., 1990. Diffusion of hydrogen in olivine: implications for water in the mantle. J. Geophys. Res. 95, 5079–5088.
Nishihara, Y., Shinmei, T., Karato, S., 2006. Grain-growth kinetics in wadsleyite: effects of chemical environment. Phys. Earth Planet. Inter. 154, 30–43.
Nishihara, Y., Shinmei, T., Karato, S., 2008. Effects of chemical environments on the hydrogen-defects in wadsleyite. Am. Mineral. 93, 831–843.
Paterson, M.S., 1982. The determination of hydroxyl by infrared absorption in quartz, silicate glass and similar materials. Bull. Mineral. 105, 20–29.
Schock, R.N., Duba, A.G., Shankland, T.J., 1989. Electrical conduction in olivine. J. Geophys. Res. 94, 5829–5839.
Tyburczy, J.A., Roberts, J.J., 1990. Low frequency electrical response of polycrystalline olivine compacts: grain boundary transport. Geophys. Res. Lett. 17, 1985–1988.
Wang, D., Mookherjee, M., Xu, Y., Karato, S., 2006. The effect of water on the electrical conductivity in olivine. Nature 443, 977–980.
Yoshino, T., Katsura, T., 2013. Electrical conductivity of mantle minerals: role of water in conductivity anomalies. Annu. Rev. Earth Planet. Sci. 41, 605–628.
Zhang, J., Li, B., Utsumi, W., Liebermann, R.C., 1996. In situ X-ray observations of the coesite–stishovite transition: reversed phase boundary and kinetics. Phys. Chem. Miner. 23, 1–10.